PHILOSOPHICAL TRANSACTIONS A

rsta.royalsocietypublishing.org

Research

Article submitted to journal

Subject Areas:
dissipative systems, extreme events, ultra-short pulses, self-organization

Keywords:
dissipative solitons, rogue waves, Ginzburg-Landau equation, bifurcations, extreme spikes

Author for correspondence:
N. Akhmediev
e-mail:
nna124@rsphysse.anu.edu.au

THE ROYAL SOCIETY PUBLISHING

Dissipative solitons with extreme spikes in the normal and anomalous dispersion regimes

N. Akhmediev[1], J. M. Soto-Crespo[2], Peter Vouzas[1], N. Devine[1] and Wonkeun Chang[3]

[1]Optical Sciences Group, Research School of Physics and Engineering, The Australian National University, Acton ACT 2601, Australia
[2]Instituto de Óptica, C.S.I.C., Serrano 121, 28006 Madrid, Spain
[3] School of Electrical and Electronic Engineering College of Engineering, Nanyang Technological University, Singapore 639798

Prigogine's ideas of systems far from equilibrium and self-organization [1,2] deeply influenced physics and soliton science in particular. It allowed us to extend the notion of solitons from purely integrable cases to the concept of dissipative solitons. The latter are qualitatively different from the solitons in integrable and Hamiltonian systems. The variety of their forms is huge. We consider here only one recent example – dissipative solitons with extreme spikes (DSES). We found that DSES exist in large regions of the parameter space of the complex cubic-quintic Ginzburg-Landau equation. A continuous variation of any of its parameters results in a rich structure of bifurcations.

1. Introduction

The dissipative soliton (DS) concept is a fundamental extension of that for solitons in conservative and integrable systems [3]. It incorporates ideas from three major sources, viz. standard soliton theory developed since the 1960s, notions from nonlinear dynamics theory and Prigogine's ideas [1,2] of systems far from equilibrium and self-organization [4] (see Fig.1(a)). These are basically the three sources and the three constituent parts of this novel paradigm. From the standard soliton theory, it takes the notion of the balance between diffraction /dispersion and nonlinearity. The concept of

dissipative soliton also requires balance between gain and loss. The latter is necessary for solitons to be robust objects. Even the slightest imbalance will result in the solution either growing indefinitely, if gain prevails, or disappearing completely in case of an excess of losses. Thus, instead of a single balance, we have to consider a composite balance between several physical phenomena [3–5] (see Fig.1(b)).

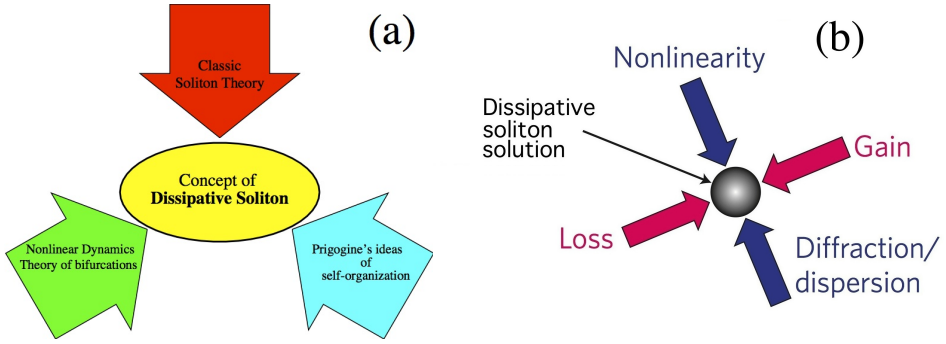

Figure 1. (a) Three sources and constituent parts of the concept of dissipative solitons [4]. (b) Composite balance as a condition for dissipative soliton existence [5]

Another essential part of the DS concept is Prigogine's theory of systems far from equilibrium [1,2]. It tells us that solitons are self-organized formations requiring a continuous supply of energy or matter or both [6]. As soon as that supply finishes, the dissipative soliton ceases to exist. In simple terms, self-organization means that for a given set of external parameters, certain initial conditions converge to a stable localized solution of the system. Thus, the final state is determined by the physical laws and not by the initial condition. For infinite-dimensional dynamical systems, this stable solution can be very complicated. It is not necessarily a smooth function with a single maximum and exponentially decaying tails. Moreover, there can be several stable solutions existing for the same set of parameters. This can even happen in the case of a relatively simple equation like the complex cubic-quintic Ginzburg–Landau equation. The majority of processes in nature are governed by far more complicated dynamics. Thus, stationary solutions of these systems can be considerably more involved.

In optics, pulse solutions of lasers systems and cavities [] constitute the most typical example of dissipative solitons. The complexity of the balance discussed above leads to a large variety of soliton profiles [7]. These include common bell-shaped solitons [8,9], flat top solitons [10], creeping solitons [11] and many other nontrivial forms [12–14]. Moreover, DS can evolve on propagation changing shape periodically, chaotically or lead to the formation of rogue waves [15,16].

One of the most unusual DS dynamics found recently is the appearance of sharp peaks on top of a more stable wider soliton [17] that serves as a background. These sharp peaks are localized in both the transversal and the longitudinal directions. Sharp peaks may appear regularly or chaotically [18]. In the latter case, they are known as spiny solitons [19]. Remarkably, these types of solitons, that we name dissipative solitons with extreme spikes (DSES), are not something exceptional. They do exist in several unconnected regions in the parameter space of the complex cubic-quintic Ginzburg-Landau equation (CGLE). Therefore, if they are a common type of CGLE solutions, they deserve further theoretical and experimental studies. Experimental studies require high-resolution measurements to resolve the narrow spikes of these solutions. In principle, the new solutions can be related to noise-like pulses [19]. Noise-like pulses have been studied

extensively [20–26] and they can serve as a bridge connecting theoretical and experimental studies on the subject of DSESs.

In contrast to solitons of Hamiltonian systems [3,27], dissipative solitons do exist no matter whether the average dispersion in the cavity is normal, anomalous or zero. Dispersion can have any sign for the total balance to remain effective for forming a localized solution. Generally, anomalous dispersion provides easier conditions for this balance because it is matched with the balance achieved for Hamiltonian solitons. Accordingly, the soliton temporal profile and spectrum are often close to sech-functions. On the other hand, when dealing with normal dispersion cavities, we may expect more exotic solutions [28–30]. The normal dispersion, as we know, is preferential when pulses with higher energy are needed [30–32]. The transition between the anomalous and normal dispersion and its effect on soliton formation is an interesting phenomenon that deserves further studies.

The study of extreme pulses in optics [33–36] is a very hot topic nowadays. These pulses with unexpectedly high amplitude appear normally in a chaotic wave field. Its study may help to understand the phenomenon of extremes as a general concept that could be applied to other fields in physics including rogue waves in the oceans [37–39]. The latter are usually associated with dangers that ocean waves may represent. In contrast, extreme pulses in optics are safe to operate with. Moreover, they can be useful in applications providing ways for increasing the amplitude and the energy of the pulses. However, in order to do this, a better understanding of extreme pulses should be reached.

2. Model

One of the most efficient techniques in modeling passively mode-locked lasers is the master equation approach [40]. This equation normally takes one or another form of the complex cubic-quintic Ginzburg-Landau equation [41,42]. The CGLE has solutions with unusual properties, such as exploding and pulsating solitons [43], creeping solitons [11], chaotic solitons [7], dissipative soliton pairs [44], dissipative rogue waves [15,16], dissipative soliton resonances [45], and even spiny solitons [19]. Many of its predictions have been later observed experimentally [8,10,12–14,29,30,46–48], thus proving the fruitfulness of the approach. The cubic-quintic complex Ginzburg-Landau equation that we are dealing with reads [5,49]:

$$i\psi_z + \frac{D}{2}\psi_{tt} + |\psi|^2\psi + \nu|\psi|^4\psi = i\delta\psi + i\epsilon|\psi|^2\psi + i\beta\psi_{tt} + i\mu|\psi|^4\psi.$$

For passively mode-locked lasers, t is the normalized time in a frame of reference moving with the group velocity, ψ is the complex envelope of the optical field and z is the propagation distance along the unfolded cavity. The meaning of the equation parameters on the left hand side is the following: D denotes the cavity dispersion, being anomalous when $D > 0$ and normal if $D < 0$, and ν is the quintic refractive index coefficient. The coefficients of the dissipative terms, written on the right-hand-side of the equation, are the following: δ denotes linear gain/loss, β is the gain bandwidth coefficient, and ϵ and μ are the cubic and quintic gain/loss coefficients, respectively.

Several types of periodic solutions to this equation with unusual behaviors have been obtained in the anomalous dispersion regime [43]. These solutions experienced periodic changes mainly in their width, while keeping almost constant their peak amplitude. In contrast, the solutions presented here change its peak amplitudes rather than its width. These amplitude variations are extreme. In fact, this specific type of evolution with sharp peaks requires a special care in numerical procedures.

3. Pulsating solitons with extreme spikes

Extreme pulsations, observed firstly in the normal dispersion regime, are characterized by narrow spikes developed on top of a roughly stationary soliton that serves as pedestal supporting these peaks. In order to characterize these solutions, we use two pulse parameters: the energy, $Q(z)$, and

the peak amplitude, $|\psi|_{peak}(z)$. They are defined as $Q(z) = \int_{-\infty}^{\infty} |\psi(z,t)|^2 dt$, and $|\psi|_{peak}(z) = max|\psi(t,z)|, \forall t$. These two functions depend only on z. For periodically pulsating solutions, the maximum and the minimum of these functions are denoted by $Q_{M,m}$ and $|\psi|_{M,m}$ respectively.

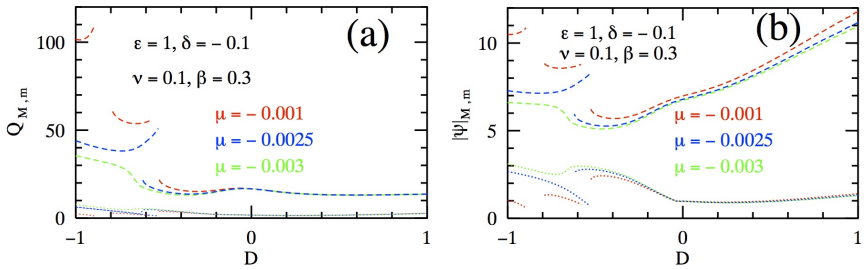

Figure 2. (a) The maximal, Q_M, (dashed curves) and minimal, Q_m, (dotted curves) soliton energy vs the cavity dispersion, D. The red curves are for $\mu = -0.001$, the blue ones for $\mu = -0.0025$ and the green for $\mu = -0.003$. The values of other equation parameters are shown inside the figure. (b) The maximal (dashed curves) and minimal (dotted curves) soliton peak amplitude vs D for the same cases.

Fig.2(a) shows the dependence of the calculated maximum (dashed lines) and minimum (dotted lines) of the energy, Q, on the cavity dispersion. Parameters of the CGLE are taken to be: $\epsilon = 1$, $\delta = -0.1$, $\nu = 0.1$, $\beta = 0.3$, while for the gain saturation, μ, we took three different values -0.001, -0.0025 and -0.003. These three values provide different bifurcation patterns. When $\mu = -0.001$ (red curves), there are three different families of pulsating solutions separated by smaller regions where no localized solutions exist. The amplitudes of the energy oscillations $Q(z)$ for these three families differ considerably. The maximum energy is above 100 for the left hand side curve (when D is close to -1) while it is below 20 for the right hand side curve (when $D > -0.5$). When $\mu = -0.0025$ there are only two families of solutions. Moreover, their regions of existence overlap. There is a small region of D-values around $D \approx -0.6$ with bistability. Finally, when $\mu = -0.003$, there is only one continuous curve for each of the values Q_m and Q_M. This means that only one branch of solitons exists in the whole interval of D-values of interest.

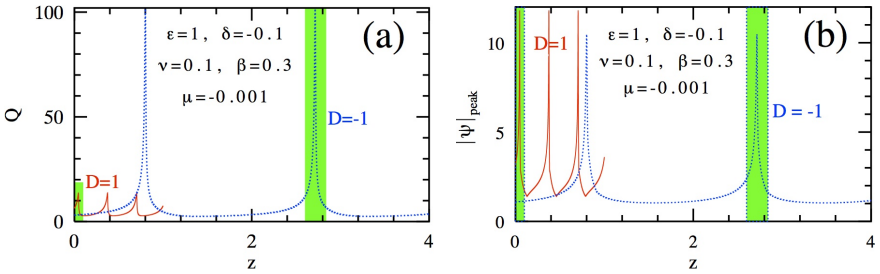

Figure 3. Evolution of (a) the energy, Q, and (b) the peak amplitude for a few periods of extreme pulse oscillations when $\mu = -0.001$, and D is either 1 or -1. In each panel, the red curve is for the anomalous case (positive D), and the blue curve is for the normal dispersion case (negative D). The two green regions mark the evolution shown in Fig.4 and Fig.5. The first (left) green region is for positive D and the second (right) green region is for negative D.

For D greater than -0.4, the $Q_{M,m}$-curves for all three values of μ nearly coincide. Moreover, these curves hardly change with D. They also exhibit a much smaller energy variation from minimum to maximum giving the impression that the pulsations are not as extreme as for the

cases around $D=-1$. However, this impression fades away when we turn our attention to the amplitude of pulsations. The maximal, $|\psi|_M$, and minimal, $|\psi|_m$, peak amplitudes for the same interval of D-values and same equation parameters are shown in Fig.2(b). They differ considerably (nearly 10 times) even in the case of anomalous dispersion as it can be seen from this figure. In this region of dispersion, the amplitude of the oscillations steadily increases with D. As the energy hardly changes, we can conclude that the spike on top of the pulse becomes narrower as D increases. For positive D, the change of μ from -0.001 to -0.003 hardly influences the solution, whereas it had a crucial influence for negative D.

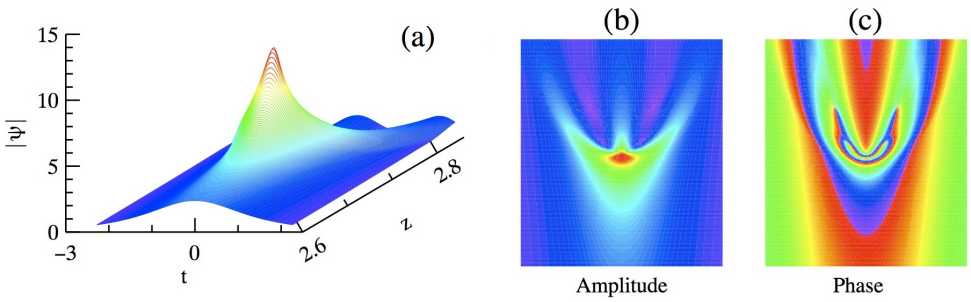

Figure 4. (a) Extreme pulse evolution for the normal dispersion case. This plot is for the r.h.s. green regions shown in Figs.3(a) and 3(b). The panels b) and c) are false color plots of the amplitude and phase of the same data.

The extremity of the pulsations is best visible in the evolution plots along the z-axis. The periodic evolution of the energy, Q, is shown in Fig.3(a) while the evolution of the peak amplitude is shown in Fig.3(b). For this demonstration, we have chosen $\mu=-0.001$ and two values of D at the opposite ends of the dispersion interval, $D=1$ (red solid curves) and $D=-1$ (blue dotted curves). We can see, from Figs.3(a) and 3(b), that the period of oscillations is long in the case of normal dispersion. The solution remains in the form of a low amplitude pedestal soliton for most of the period with the spike occupying a small part of the period. On the contrary, the period becomes shorter in the case of anomalous dispersion so that the duration of the spikes is now comparable to the period. The energy, Q, oscillates with stronger magnitude when $D=-1$. These oscillations are almost ten times smaller when $D=+1$. However, the oscillations of the peak amplitude in the two cases are comparable as can be seen from Fig.3(b).

3D-plots of the pulse evolution around an extreme peak are shown in Fig.4 for the case of normal dispersion and in Fig.5 for the anomalous dispersion case. Each plot shows the evolution within the z-interval highlighted by the green shaded rectangles in Figs.3(a) and 3(b). The panel (a) in each figure is the amplitude profile of the pulse in the (t,z)-plane while the panels (b) and (c) show false-color plots of the pulse amplitude and phase respectively on the same (t,z)-plane. For $D=1$ (anomalous dispersion case), the extreme peak is much narrower and significantly shorter than in the case of normal dispersion. This becomes clear if we look at the different scales used in the two figures both in t and z directions. The phase shows a more complicated structure in the normal dispersion case, which is related to a more involved spectrum.

4. Bifurcation diagrams

DSES solutions occupy a significant region in the space of parameters of the CGLE. We can vary any of the CGLE parameters in relatively wide intervals and the solutions still have their distinctive features. In the previous section, we studied the influence of D on the DSES. Now we shall illustrate the enormity of the size of the area of existence of DSESs, by changing ϵ and β. Each of these parameters can be changed in relatively wide intervals and the solutions stay

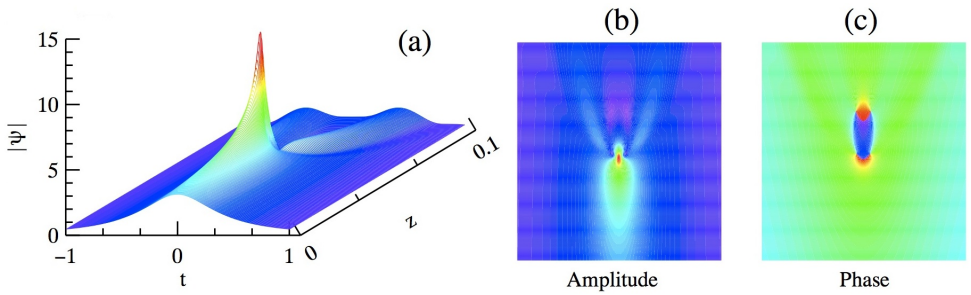

Figure 5. a) Extreme pulse evolution for the anomalous dispersion case. This plot is for the l.h.s. green regions shown in Figs.3(a) and 3(b). The panels b) and c) are the false color plots of the amplitude and the phase of the same data.

in the form of DSESs. Of course, the particular shape of these DSESs changes with the change of the equation parameters. Moreover, their dynamics may change from periodic pulsations to other types of evolution including chaotic behavior. Qualitative changes take the form of bifurcations. There are many bifurcations in each interval that we considered. In the simplest case, a bifurcation is a transition from a stationary solution to a pulsating solution of DSES type. The most standard DSES exhibits one single centered spike per period. But, changing a parameter these pulsating solutions transform into more complicated DSES with several spikes per period or with asymmetric profiles.

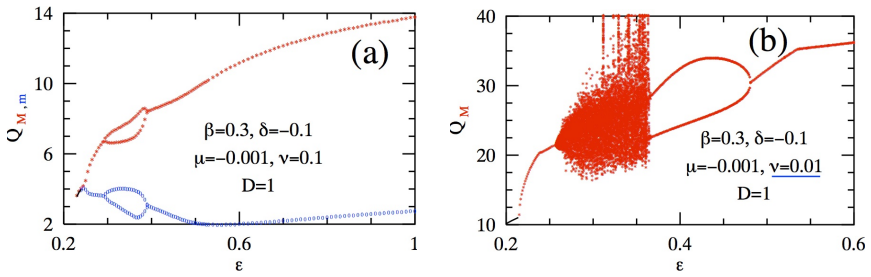

Figure 6. Two bifurcation diagrams obtained when ϵ is varied [50]. The plot in (a) shows the maxima and minima of the energy Q. It starts with $\epsilon = 0.23$ where $Q_M = Q_m$. This corresponds to a stationary soliton without spikes. The first bifurcation at $\epsilon \approx 0.25$ leads to a pulsating soliton with a single spike per period. The bifurcation at $\epsilon \approx 0.3$ leads to a pulsating soliton with two spikes per period. These return back to pulsations with a single spike per period at $\epsilon \approx 0.4$. The second diagram (b) shows only maxima of Q. The central part between the two inflection points correspond to asymmetric DSESs.

The above mentioned types of solutions have been obtained by varying, for instance, the parameter ϵ in the CGLE. Figure.6(a) shows a typical bifurcation diagram obtained this way. The upper (red) curve describes the maxima of energy while the lower (blue) curve corresponds to the minima. The region $0.3 \leq \epsilon \leq 0.4$ corresponds to double spike generation per period. The splitting of the curves on the diagram demonstrates two different values of energy of the two spikes. The areas beyond this interval correspond to solutions having a single spike in each period. In the interval $[0.23, 0.25]$, maxima and minima of solitons merge into a single curve. This means that the pulsating DSES is transformed into a stationary soliton without spikes. At values of ϵ smaller than 0.23, soliton solutions become unstable and vanish on propagation.

Changing for instance the value of ν, the bifurcation diagram may become more involved as Fig.6(b) shows. Here for the sake of clarity only maxima of Q are shown. The inflection point at $\epsilon \approx 0.55$ corresponds to symmetry breaking. Below this point DSES solutions lose temporal symmetry and start to move. The bifurcation at $\epsilon \approx 0.48$ corresponds to a transition to solitons with two spikes per period. Further reduction of ϵ below ≈ 0.36 switches to a chaotic dynamics. Non-moving DSES with one spike per period are restored at $\epsilon \approx 0.25$. These are asymmetric solutions with the profile inverted after every period. Below the inflection point, at $\epsilon = 0.24$, the DSES fully recover their temporal symmetry. For ϵ less than 0.215, the solution is transformed into a stationary soliton. A typical example of asymmetric DSES with two spikes per period is shown in Fig.7(a). This plot shows explicitly the asymmetry and the motion of the soliton with spikes. The velocity of motion is fixed once the equation parameters are fixed. The soliton is asymmetric in two ways. Firstly, the “mother" soliton is asymmetric. Secondly, the location of the spikes is asymmetric relative to the “mother" soliton. The evolution of the peak amplitude for this solution is shown in Fig.7(b) while the evolution of the energy is shown in Fig.7(c).

The main difference from the case shown in Fig.5 is the higher modulation depth. Namely, the extreme amplitudes here are much higher than in Fig.5 and much higher than the amplitude of the “mother" soliton.

An important observation is that the interval of DSES existence here is also very large. It extends from $\epsilon = 0.215$ to $\epsilon > 0.6$. This is a very large interval for the cubic gain term.

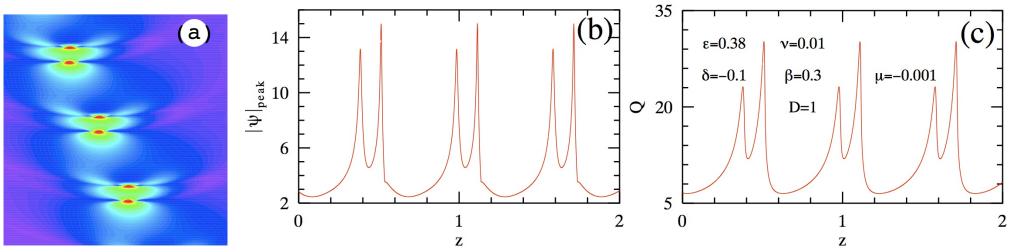

Figure 7. Moving DSES with two spikes per period [50]. (a) False color plot of the amplitude on the (t, z)-plane. (b) Evolution of the peak amplitude. (c) Evolution of the energy Q. Parameters of the CGLE are given in the panel (c).

Next, we took $\nu = 0.01$ and varied β keeping all other parameters fixed. The corresponding bifurcation diagram is shown in Fig.8(a). We have changed β below the original point 0.3 up to 0.15 and above it up to 0.65. This whole interval contains DSES solutions. As before, for the sake of clarity and in order to keep high resolution along the vertical scale only the maxima of energy are shown. This diagram shows a rich bifurcation structure of solutions. The yellow region of (a) is further magnified in (b). This part of the diagram shows that the two main spikes experience a sequence of period doubling bifurcations before entering a region of chaotic dynamics. In order to reveal the nature of the solutions that correspond to each branch of the diagram, we present one example for each branch in Fig.9. They show the evolution of the peak amplitude. The points of β that are chosen as representative of the type of solutions of the corresponding branch are shown by blue dashed vertical lines. A small region around $\beta = 0.33$ shows up hysteresis with the corresponding bistability. The second solution in the bistability region is represented by blue points.

The case $\beta = 0.18$ corresponds to a periodic solution with two spikes per period. The case $\beta = 0.2$ is also a pulsating solution but the period of pulsations takes chaotic values. Thus, the solution is now chaotic but remains to be a single soliton. The case $\beta = 0.4$ corresponds to a pulsating DSES with 4 extreme spikes per period. This is clear both from the bifurcation diagram in Fig.8 and from the evolution curve in Fig.9. At $\beta = 0.47$, after another bifurcation, the solution returns to a periodic one with two extreme spikes per period. Two other cases $\beta = 0.505$ and $\beta = 0.52$

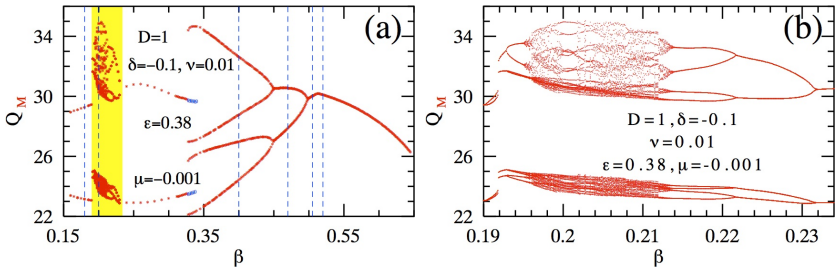

Figure 8. (a) Bifurcation diagram with β as the variable parameter [50]. The part of the diagram highlighted in yellow is magnified in (b).

correspond to pulsating solutions with one extreme peak per period. Although they look similar, these two solutions belong to different branches. This can be seen from the bifurcation curve in Fig.8. There is an inflection point on the curve located between the two cases at $\beta \approx 0.51$. It separates oscillating DSESs from symmetric ones with zero velocity. The period of oscillating solutions is twice the period of the curve $Q(z)$ seen in Fig.9. Similar inflection points can be seen on other bifurcation diagrams.

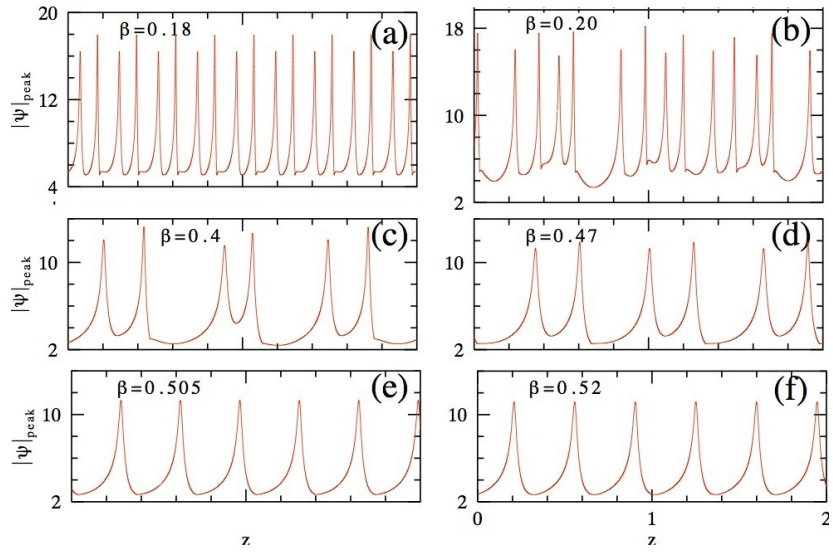

Figure 9. Evolution of the peak amplitude for the six cases (a-f) marked in Fig.8 by blue dashed vertical lines [50]. Each panel has a different vertical length but the same scale.

The most striking feature of the diagram in Fig.8 is the multiplicity of bifurcations that takes place in a relatively narrow range of parameter change. This fact confirms that the CGLE has a myriad of different types of solutions. There are periodic and chaotic solutions in this region. The chaotic region can be entered through a sequence of period doubling bifurcations. This sequence can be seen in the region $0.216 < \beta < 0.231$. Other routes to chaos also exist at around $\beta = 0.201$.

5. Conclusions

The appearance of extreme spikes on top of wider dissipative solitons is a striking phenomenon that deserves further studies both theoretical and experimental. Extreme spikes can appear regularly [17] or chaotically [18]. In the latter case, they can be considered as rogue waves [19]. Extreme spikes can appear for a wide range of the system parameters. This range of parameters includes continuous change of the dispersion parameter of the cavity from normal to anomalous. Remarkably, the anomalous dispersion case provides considerably sharper spikes than the normal dispersion one. When building lasers generating ultra-short pulses, this can be considered as an advantage.

Spikes occupy significant volumes of the parameter space of the complex cubic-quintic Ginzburg-Landau equation. Variation of any of the five parameters in this space results in a rich structure of bifurcations. Bifurcation diagrams reveal periodic and chaotic dynamics of DSES. Periodic solutions may have one or several pairs of spikes per period. They can be centered in t, oscillating around a fixed t, moving with a fixed or variable velocity, and even along a zigzag trajectory. Transition between them can take the form of bifurcations.

Funding. The work of JMSC was supported by MINECO under contract TEC2015-71127-C2-1-R, and by C.A.M. under contract S2013/MIT-2790. The three authors, P.V., W.C. and N.A., acknowledge the support of the Australian Research Council (DE130101432 and DP150102057). JMSC and NA also acknowledge the support of the Volkswagen Foundation.

References

1. Prigogine I. and Lefever R. 1968. *Symmetry Breaking Instabilities in Dissipative Systems*. J. Chem. Phys. **48**, 1695.
2. Glansdorff P. and Prigogine I. 1971. *Thermodynamic Theory of Structures, Stability and Fluctuations*. Wiley, New York, London.
3. Akhmediev N. and Ankiewicz A. 2003. *Solitons around us: Integrable, Hamiltonian and Dissipative systems, Chapter in book: Optical Solitons: Theoretical and Experimental Challenges*, Ed. by Porsezian K. and Kurakose V. C., Springer, Berlin-Heidelberg, pp. 105-126.
4. N. Akhmediev N. and A. Ankiewicz A. (Eds.). 2005. *Dissipative Solitons, Lecture Notes in Physics* **661**, Springer, Berlin-Heidelberg.
5. Grelu Ph. and Akhmediev N. 2012. Dissipative solitons for mode-locked lasers, *Nature Photonics* **6**, 84.
6. Akhmediev N., Soto-Crespo J. M. and Brand H. R. 2013. Dissipative solitons with energy and matter flows: Fundamental building blocks for the world of living organisms, *Phys. Lett. A* **377**, 968.
7. Akhmediev N., Soto-Crespo J. M., and Town G. 2001. Pulsating solitons, chaotic solitons, period doubling, and pulse coexistence in mode-locked lasers: Complex Ginzburg-Landau equation approach, *Phys. Rev. E* **63**, 056602.
8. Kieu K., Renninger W. H., Chong A., and Wise F. W. 2009. Sub-100 fs pulses at watt-level powers from a dissipative-soliton fiber laser, *Opt. Lett.* **34**, 593.
9. Chen H., Heng S. P., Jiang Z. F., Hou J. 2016. 80 nJ ultrafast dissipative soliton generation in dumbbell-shaped mode-locked fiber laser, *Opt Lett.* **41**, 4210.
10. Zhao L. M., Bartnik A. C., Tai Q. Q. and Wise F. W. 2013. Generation of 8-nJ pulses from a dissipative-soliton fiber laser with a nonlinear optical loop mirror, *Phys. Rev. E* **38** 1942 – 1944.
11. Chang W., Ankiewicz A. and Akhmediev N. 2007. Creeping solitons of the complex Ginzburg–Landau equation with a low-dimensional dynamical system model, *Phys. Lett. A* **362**, 31–36.
12. Cuadrado-Laborde C., Armas-Rivera I., Carrascosa A., Kuzin E. A., Beltrán-Pérez G., Díez A., and Andrés M. V. 2016. Instantaneous frequency measurement of dissipative soliton resonant light pulses, *Opt. Lett.* **41**, 5704.
13. Amrani F., Haboucha A., Salhi M., Leblond H., Komarov A. and Sanchez F. 2010. Dissipative solitons compounds in a fiber laser: Analogy with the states of the matter, *Appl. Phys. B* **99**, 107.
14. Kharenko D. S., Shtyrina O. V., Yarutkina I. A., Podivilov E. V., Fedoruk M. P., and Babin S. A. 2011. Highly chirped dissipative solitons as a one-parameter family of stable solutions of the cubic-quintic Ginzburg-Landau equation, *J. Opt. Soc. Am. B* **28**, 2314.

15. Soto-Crespo J. M., Grelu Ph. and Akhmediev N. 2011. Dissipative rogue waves: Extreme pulses generated by passively mode-locked lasers, *Phys. Rev. E* **84**, 016604.
16. Zaviyalov A., Egorov O., Iliew R. and Lederer F. 2012. Rogue waves in mode-locked fiber lasers, *Phys. Rev. A* **85**, 013828.
17. Chang W., Soto-Crespo J. M., Vouzas P. and Akhmediev N. 2015. Extreme amplitude spikes in a laser model described by the complex Ginzburg-Landau equation, *Opt. Lett.* **40**, 2949 – 2952.
18. Chang W., Soto-Crespo J. M., Vouzas P. and Akhmediev N. 2015. Extreme soliton pulsations in dissipative systems *Phys. Rev. E* **92**, 022926.
19. Chang W., Soto-Crespo J. M., Vouzas P. and Akhmediev N. 2015. Spiny solitons and noise-like pulses, *J. Opt. Soc. Am.* **32**, 1377 – 1383.
20. Horowitz M., Barad Y., and Silberberg Y. 1997. Noiselike pulses with a broadband spectrum generated from an erbium-doped fibre laser, *Opt. Lett.* **22**, 799.
21. Zhao L. M., Tang D. Y., Cheng T. H., Tam H. Y., and Lu C. 2008. 120 nm bandwidth noise-like pulse generation in an erbium-doped fiber laser, *Opt. Commun.* **281**, 157.
22. Runge A. F. J., Aguergaray C., Broderick N. G. R. and Erkintalo M. 2013. Coherence and shot-to-shot spectral fluctuations in noise-like ultrafast fiber lasers, *Opt. Lett.* **38**, 4327.
23. Kang J. U. 2000. Broadband quasi-stationary pulses in mode-locked fiber ring laser, *Opt. Commun.* **182**, 433.
24. Pottiez O., Grajales-Coutino R., Ibarra-Escamilla B., Kuzin E. A. and Hernández-García J. C. 2011. Adjustable noiselike pulses from a figure-eight fiber laser, *Appl. Opt.* **50**, E24.
25. Horowitz M. and Y. Silberberg Y. 1998. Control of noiselike pulse generation in erbium-doped fiber lasers, *IEEE Photonic. Tech. L.* **10**, 1389.
26. Boucon A., Barviau B., Fatome J., Finot C., Sylvestre T., Lee M. W., Grelu Ph., and Millot G. 2012. Noise-like pulses generated at high harmonics in a partially-mode-locked km-long Raman fiber laser, *Appl. Phys. B* **106**, 283.
27. Mollenauer L. F. and Gordon G. P. 2006. *Solitons in optical fibres*, Elsevier, London.
28. Renninger W. H., Chong A. and Wise F. W. 2008. Dissipative solitons in normal-dispersion fiber lasers, *Phys. Rev. A* **77**, 023814.
29. Liu X. 2009. Numerical and experimental investigation of dissipative solitons in passively mode-locked fiber lasers with large net-normal-dispersion and high nonlinearity, *Opt. Express* **17**, 22401.
30. Chichkov B., Hausmann K., Wandt D., Morgner U., Neumann J., Kracht D. 2010. High-power dissipative solitons from an all-normal dispersion erbium fiber oscillator, *Opt. Lett.* **16**, 2807.
31. Chong A., Buckley J., Renninger W. H. and Wise F. W. 2006. All-normal-dispersion femtosecond fiber laser, *Opt. Express* **14**, 21.
32. Chong A., Renninger W. H. and Wise F. W. 2007. All-normal-dispersion femtosecond fiber laser with pulse energy above 20 nJ, *Opt. Lett.* **32**, 16.
33. Solli D. R., Ropers C., Koonath P. and Jalali B. 2007. *Nature* **450**, 1054.
34. Akhmediev N., Dudley J. M., Solli D. R. and Turitsyn S. K. 2013. Recent progress in investigating optical rogue waves, *J. Opt.* **15**, 060201.
35. Dudley J. M., Dias F., Erkintalo M. and Genty G. 2014. Instabilities, breathers and rogue waves in optics, *Nature Photonics* **8**, 755 – 764.
36. Akhmediev N. et al. 2016. Roadmap on optical rogue waves and extreme events, *J. Opt.* **18**, 063001.
37. Osborne A.. 2010. *Nonlinear Ocean Waves & the Inverse Scattering Transform*. Academic Press.
38. Kharif C., Pelinovsky E., and Slunyaev A. 2009. *Rogue Waves in the Ocean*, Springer.
39. Müller P., Garrett C. and Osborne A. 2005, *Oceanography* **18**, 66.
40. Haus H. A.2000. Mode-locking of lasers, *IEEE J. Selected Topics in Quant. Electron.* **6**, 1173.
41. Komarov A., Leblond H. and Sanchez F. 2005. Quintic complex Ginzburg-Landau model for ring fiber lasers, *Phys. Rev. E* **72**, 025604(R).
42. Moores J. D. 1993. On the Ginzburg-Landau laser mode-locking model with fifth-order saturable absorber term, *Opt. Commun.* **96**, 65.
43. Soto-Crespo J. M., Akhmediev N. and Ankiewicz A. 2000. Pulsating, creeping and erupting solitons in dissipative systems, *Phys. Rev. Lett.* **85**, 2937.
44. Akhmediev N., Ankiewicz A. and Soto-Crespo J. M. 1998. Stable soliton pairs in optical transmission lines and fiber lasers, *J. Opt. Soc. Am. B* **15** 515 – 523.
45. Grelu Ph., Chang W., Ankiewicz A., Soto-Crespo J. M. & Akhmediev N. 2010. Dissipative soliton resonance as a guideline for high-energy pulse laser oscillators, *JOSA B* **27**, 2336.

46. Mortag D., Wandt D., Morgner U., Kracht D. and Neumann J. 2011. Sub-80-fs pulses from an all-fiber-integrated dissipative-soliton laser at 1 μm, *Opt. Express* **19**, 546.
47. Grelu Ph., Belhache F., Gutty F. and Soto-Crespo J. M. 2002. Phase-locked soliton pairs in a stretched-pulse fiber laser, *Opt. Lett.* **27**, 966 – 968.
48. Cundiff S. T., Soto-Crespo J. M. and Akhmediev N. 2002. Experimental evidence for soliton explosions, *Phys. Rev. Lett.* **88**, 073903.
49. Korytin A. I., Kryachko A. Yu. and Sergeev A. M. 2001. Dissipative solitons in the complex Ginzburg-Landau equation for femtosecond lasers, *Radiophys. Quant. Electron.* **44**, 428.
50. Soto-Crespo J. M., Devine N. and Akhmediev N. 2017 Dissipative solitons with extreme spikes: bifurcation diagrams in the anomalous dispersion regime, *JOSA B* **34**, 1542.